Dynamical bistability in the driven circuit QED

V. Peano[1,3] and M. Thorwart[2,3]

[1] *Physikalisches Institut, Universität Freiburg, 79104 Freiburg, Germany*
[2] *Freiburg Institute for Advanced Studies (FRIAS), Universität Freiburg, 79104 Freiburg, Germany*
[3]*Institut für Theoretische Physik, Heinrich-Heine-Universität Düsseldorf, 40225 Düsseldorf, Germany*
(Dated: March 13, 2009)

We show that the nonlinear response of a driven circuit quantum electrodynamics setup displays antiresonant multiphoton transitions, as recently observed in a transmon qubit device. By including photon leaking, we explain the lineshape by a perturbative and a semiclassical analysis. We derive a bistable semiclassical quasienergy surface whose groundstate is squeezed, allowing for a squeezing-dependent local effective temperature. We study the escape dynamics out of the metastable state and find signatures of dynamical tunneling, similar as for the quantum Duffing oscillator.

One of the nontrivial fundamental models of quantum physics is the Jaynes-Cummings (JC) model [1]. It was introduced to describe the interaction of a two-level atom and a single quantized electromagnetic field mode. Being sufficiently simple, its dynamics is very rich though, including Rabi oscillations, collapse and revival phenomena, squeezing, entanglement, Schrödinger cat and Fock states, and photon antibunching [2]. Beyond quantum optical set-ups, it is applicable to many situations of nanocircuit quantum electrodynamics (QED), such as Cooper pair boxes [3], superconducting flux qubits [4], Josephson junctions [5], and semiconductor quantum dots [6]. In particular, the latter setups allow to explore the regime of strong coupling and nonlinear response.

Recently, unique nonlinear features have been detected in the transmitted heterodyne signal of a superconducting transmon qubit device [7]. For weak driving, the two well-known vacuum Rabi resonances reflect transitions between the groundstate and the first/the second excited state of the undriven JC spectrum. Their difference in energy is $2\hbar g$, where g is the interaction strength of the qubit and the harmonic mode. For increasing driving, each vacuum Rabi peak supersplits into additional (anti-)resonances with the characteristic $\sqrt{n}$ spacing. The measurements have been corroborated with accurate numerical simulations [7].

In this Letter, we provide a complete physical picture for the nonlinear response of the driven JC model in terms of quantum multiphoton (anti-)resonances. The underlying physical mechanism is revealed by perturbative arguments in the rotating frame in presence of photon leaking. The lineshape is determined by the ratio of the Rabi frequency and the dissipation strength, allowing for a direct experimental control. Beyond the perturbative regime, we derive a semiclassical quasienergy surface which is bistable. Its groundstate is an amplitude squeezed state and displays large out-of-phase oscillations. It is significantly populated at a multiphoton (anti)resonance, and is metastable away from resonance. The dissipative dynamics at zero temperature involves quantum activation [8, 9], but also shows dynamic resonant tunneling [10]. Furthermore, we reveal

topological analogies with the quantum Duffing oscillator [10, 11, 12, 13].

We start from a harmonic oscillator with frequency ω which is coupled with strength g to a qubit and which is driven with frequency ω_{ex} and field strength f. In the frame rotating with ω_{ex} and for $\delta\omega \equiv \omega - \omega_{\text{ex}}, g, f \ll \omega$, we perform a rotating-wave approximation and obtain the Hamiltonian of the driven JC model ($\hbar = k_B = 1$)

$$H_{\text{JC}} = \delta\omega a^\dagger a + \frac{\delta\omega}{2}\sigma_z + \frac{g}{2}(a^\dagger\sigma_- + a\sigma_+) + \frac{f}{2}(a^\dagger + a)\,, \quad (1)$$

with $\sigma_\pm = \sigma_x \pm i\sigma_y$. Here, σ_j are the Pauli matrices. The undriven JC model has the quasienergies $\varepsilon_0 = -\delta\omega/2$, $\varepsilon_{n,\pm} = (n - 1/2)\delta\omega \pm g\sqrt{n}/2$ and the quasienergy states $|\phi_0\rangle = |0, g\rangle$, $|\phi_{n\pm}\rangle = (|n - 1, e\rangle \pm |n, g\rangle)/\sqrt{2}$. We will refer to latter as n-photon dressed states with two spin directions $\pm$. For $f \neq 0$, avoided crossings of the quasienergy levels arise, which correspond to N-photon transitions at $\delta\omega = \pm g/(2\sqrt{N})$. To have well separated resonances, we consider the regime $g \ll f$. Around the resonance, the eigenstates (at leading order) are $|\phi_0^f\rangle \simeq \cos\frac{\theta}{2}|\phi_0\rangle - \sin\frac{\theta}{2}|\phi_{N\pm}\rangle$, $|\phi_{N\pm}^f\rangle \simeq \sin\frac{\theta}{2}|\phi_0\rangle + \cos\frac{\theta}{2}|\phi_{N\pm}\rangle$, with $\tan\theta = -\Omega_N/(\omega_{\text{ex}} - \omega_{N\pm})$ with the Rabi frequency $\Omega_N \propto f^N/g^{N-1}$.

To incorporate dissipative effects on the level of the RWA, and for low temperatures $T \ll \omega_{\text{ex}}$, we use a Lindblad master equation for the density operator $\dot\rho = -i[H, \rho] + \mathcal{L}\rho$ with $\mathcal{L} = \gamma\left([a\rho, a^\dagger] + [a, \rho a^\dagger]\right)/2$. Then, only photon leaking from the system into the bath is possible. Hence, in absence of multiphoton transitions, $|\phi_0\rangle$ is dominantly populated in the stationary state. In contrast, at a multiphoton resonance, the stationary state is generated by coherent driving to the N-photon state and a subsequent relaxation via all the intermediate n-photon states to the 0-photon state due to photon leaking. Eventually, this nontrivial interplay generates a stationary mixture of all n-photon states ($n \leq N$).

We are interested in the nonlinear response characterized by $\langle a \rangle = \text{tr}(\varrho a) = Ae^{i\varphi} = \sum_{\alpha\beta}\varrho_{\alpha\beta}a_{\beta\alpha}$. We discuss the case $\delta\omega > 0$, the opposite follows from $|\phi_{n\pm}\rangle \rightarrow |\phi_{n\mp}\rangle$, $f \rightarrow -f$ and $\varphi \rightarrow -\varphi + \pi$. The modulus is related to the experimentally accessible transmission
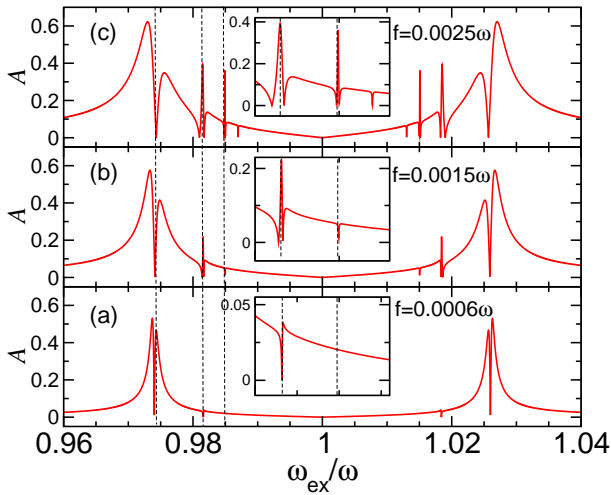
FIG. 1: Amplitude A as a function of the driving frequency ω_{ex} for $f = 0.0006$ (a), $f = 0.0015$ (b) and $f = 0.0025$ (c). Insets: zooms to the corresponding (anti-)resonances marked by the dashed lines. Moreover, $g = 0.052\omega, \gamma = 5 \times 10^{-5}\omega$.
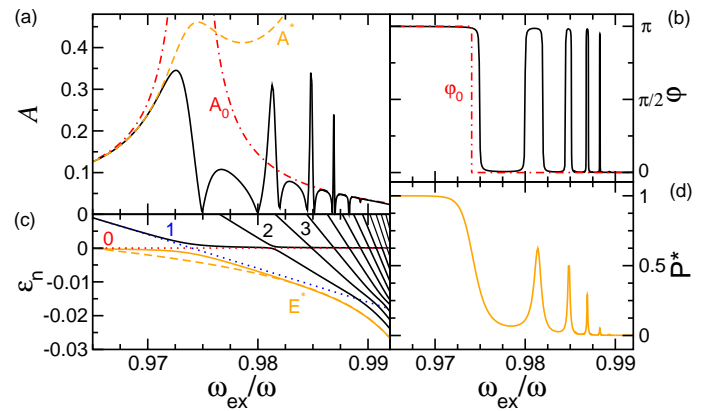

FIG. 2: Nonlinear response of the driven JC model: (a) amplitude, (b) phase, (c) quasienergies, and (d) population of the lowest quasienergy state $|\psi^*\rangle$ for $g = 0.052\omega, f = 0.004\omega, \gamma = 10^{-4}\omega$. Dashed-dotted red line in (a,b): lowest-order result for non-resonant approximation. Dashed orange line in (a): $A^* = |\langle\psi^*|a|\psi^*\rangle|$; and in (c): semiclassical result Eq. (4) for the lowest quasienergy E^*.

amplitude $\sim A$ and intensity $\sim A^2$ [7]. In the rotating frame, $\langle a\rangle < 0$ ($\varphi = \pi$) corresponds to an oscillation out of phase with respect to the drive.

The nonlinear response, in the first instance obtained from a numerical solution, is shown in Fig. 1 for the parameters corresponding to the experiment of Ref. [7]. The drive induces a splitting of the vacuum Rabi resonance and produces two families of peaks which are symmetric with respect to $\omega_{ex} = \omega$ and which are associated to the $\pm$ quasienergy states. In each family, (anti)resonances occur which correspond to multiphoton transitions and which are associated to the avoided crossings of quasienergy levels, see Fig. 2c. We note that no antiresonances occur in the photon number $\langle a^\dagger a\rangle$ [14].

For weak driving (Fig. 1a), only the 1-photon antiresonance is well pronounced. It can be described [7, 13] by a model involving the 0- and the 1-photon state. At resonance, they are equally populated and oscillate with opposite phase yielding zero response. Slightly away from resonance, one of the two states is more populated and a finite response arises. Far away from the resonance, the response again approaches zero. Overall, the lineshape of an antiresonance arises. The antiresonance around $\omega_{ex} \approx 0.98\omega$ corresponds to a 2-photon process (Fig. 1a). This feature also follows from a two state description. The shape is different from the 1-photon antiresonance, due to the background contribution of nonresonant 1-photon mixing processes[11].

For increasing driving, unexpected features arise. The multiphoton antiresonances turn into resonances, see Fig. 1b and c. Associated to the behavior of A are jumps in the phase φ, see Fig. 2b. This already suggests that two quasienergy states - one oscillating in and one out of phase - are alternatingly populated. Interestingly, the population (Fig. 2d) of the state $|\psi^*\rangle$ with lowest

quasienergy shows peaks at the resonance frequencies. In fact, as we will show below, $|\psi^*\rangle$ is localized in the bottom of a well of a bistable quasienergy surface. $|\psi^*\rangle$ is metastable since the bath induces transitions to higher quasienergies states and an escape is always possible, even at zero temperature. This feature has also been reported for the quantum Duffing oscillator [10, 12, 13].

These observations are further substantiated by perturbative arguments. Out of resonance, $\rho_{00} \simeq 1$ yielding $\langle a\rangle = \langle\phi_0^f|a|\phi_0^f\rangle \simeq \frac{f}{4}\frac{1}{-\delta\omega-g/2} + \frac{f}{4}\frac{1}{-\delta\omega+g/2}$. As follows from Figs. 2 a) and b) (dashed-dotted red lines), the lowest order response A_0 coincides with the exact one away from resonance. Moreover, $\varphi_0 = \pi$ for $\delta\omega \leq g/2$ and $\varphi_0 = 0$ for $\delta\omega > g/2$.

At the N-photon-resonance, the system tunnels from $|\phi_0\rangle$ to $|\phi_{N-}\rangle$ with probability Ω_N and the bath induces decays from $|\phi_{n-}^f\rangle \simeq |\phi_{n-}\rangle$ to $|\phi_{n-1-}^f\rangle \simeq |\phi_{n-1-}\rangle$ along the ladder $N \rightarrow N - 1 \rightarrow ... \rightarrow 1 \rightarrow 0$. The decay rates (in secular approximation) are $\mathcal{L}_{n-,(n-1)-} = (\sqrt{n} + \sqrt{n-1})^2\gamma/4$ for $n \neq 1$ and $\mathcal{L}_{1-,0} = \gamma/2$. Hence, the rate from the 1-photon to the 0-photon state is smallest. Note that the probability of a decay to a state with opposite spin is small, i.e., $\mathcal{L}_{(n-1)-,n+}/\mathcal{L}_{(n-1)+,n+} \simeq 1/[16n(n-1/2)]$. Hence, the population of the 1-photon state is always larger than those of the n-photon states. In addition, depending on the ratio γ/Ω_N, qualitatively different stationary populations arise from a competition between tunneling from $|\phi_0\rangle$ to the top of the ladder, $|\phi_{N-}\rangle$, and relaxation down the ladder. For $\gamma \gg \Omega_N$, the population of $|\phi_0\rangle$ is $\simeq 1$, because damping is more efficient than tunneling. Dissipation then completely washes out the resonance, and the response is the same as that off resonance and thus is in phase with the drive. For $\gamma \simeq \Omega_N$, a small population ρ_{11} emerges, contributing
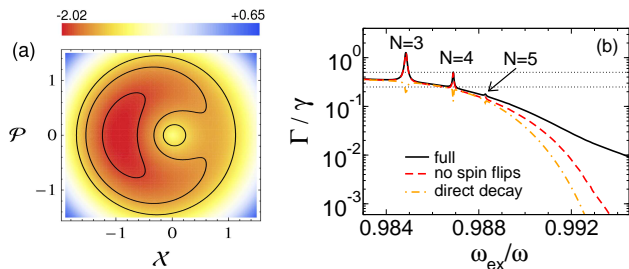
FIG. 3: (a): Quasienergy surface $Q(\mathcal{X}, \mathcal{P})$ for $g = 0.052\omega$, $f = 0.004\omega, \gamma = 10^{-4}\omega$ and $\delta\omega = 0.01\omega$ ($T_{\text{eff}} = 0.65$). (b) Solid line: Smallest eigenvalue of the Lindblad master equation. Dashed red line: the same without dissipative spin flips. Dashed-dotted orange line: decay rate for $|\psi^*\rangle \to |\phi_0^f\rangle$. Dottes lines correspond to $\gamma/2$ and $\gamma/4$.

$\rho_{11}a_{11}$ with $a_{11} = \frac{f}{2(\varepsilon_{1-} - \varepsilon_{2-})}\frac{3+2\sqrt{2}}{4} + \frac{f}{4(\varepsilon_{1-} - \varepsilon_0)} < 0$ since, in the perturbative regime and for $N < 6$, $\varepsilon_{1-} < \varepsilon_{2-}, \varepsilon_0$. This leads to a reduced response, forming an antiresonance, see, e.g., the 2-photon antiresonance shown in Fig. 1a. For $\gamma \ll \Omega_N$, tunneling is faster than relaxation and the population of $|\phi_{1-}\rangle$ becomes the largest. Then, the contribution $\rho_{11}a_{11} < 0$ dominates, leading to an overall out-of-phase oscillation. For the 2-photon resonance of Fig. 1, $\gamma/\Omega_2 = \sqrt{2}\gamma f^2/g = 2.6$ (a), 0.42 (b) and 0.15 (c).

For increasing driving, the response is qualitatively similar, although the perturbative approach becomes inadequate. In fact, as shown in Fig. 2d, at resonance, there is a large population P^* of the lowest quasienergy state $|\psi^*\rangle$. As follows from Fig. 2c, $|\psi^*\rangle \neq |\phi_{1-}\rangle$. In order to account for the importance of $|\psi^*\rangle$, we perform next a semiclassical analysis. We transform the JC eigenstates into product states $|n\sigma\rangle$ (with $\sigma = g, e$) to decouple oscillator and spin by the unitary transformation $R = \exp(\frac{-\pi}{4\sqrt{a^\dagger a + \sigma_z + 1/2}}[a^\dagger\sigma_- - a\sigma_+])$, yielding

$$\tilde{H} = |\delta\omega|\left(a^\dagger a + \sigma_z\right) + g\sigma_z\sqrt{a^\dagger a + \sigma_z + 1/2} \quad (2)$$

for the undriven JC Hamiltonian, while $\tilde{a} = R^\dagger a R = a - a\frac{1}{4(a^\dagger a + 1/2)}(1 + \sigma_x) + \mathcal{O}(n^{-3/2})$. Hence, as expected, the driving as well as the bath-induced relaxation induce spin flip transitions between dressed states. Next, we introduce the canonical variables $\mathcal{X} = \sqrt{\lambda/2}(a^\dagger + a)$ and $\mathcal{P} = i\sqrt{\lambda/2}(a^\dagger - a)$, where $\lambda = |\delta\omega|/g$ is a dimensionless parameter playing the role of $\hbar$. Eventually, neglecting the spin flips and higher order terms, we obtain the transformed Hamiltonian $\tilde{H} \simeq gQ(\mathcal{X}, \mathcal{P})$ with

$$Q(\mathcal{X}, \mathcal{P}) = \frac{\mathcal{X}^2}{2} + \frac{\mathcal{P}^2}{2} + \frac{\sigma_z}{\sqrt{\lambda}}\sqrt{\frac{\mathcal{X}^2}{2} + \frac{\mathcal{P}^2}{2}} + \frac{f}{g\sqrt{2\lambda}}\mathcal{X} \quad (3)$$

It can be interpreted as a quasienergy surface in phase space, see Fig. 3a for the qubit groundstate ($\sigma_z = -1$). The corresponding quasiclassical orbits encircle the inner maximum on an external and an internal domain. In addition, there is a range of quasienergies where two orbits

are degenerate and a dynamical bistability occurs. The surface for $\sigma_z = +1$ is a less interesting monotoneous function (not shown). The drive induces a tilt generating one stable orbit close to the quasienergy minimum. The orbits near the inner maximum correspond to small photon numbers and are not accurately described by the semiclassical approach.

Let us next consider the dynamics around the minimum at $\mathcal{P}_{\min} = 0$ and $\mathcal{X}_{\min} = -(f/g + 1/2)/\sqrt{2\lambda}$. A harmonic expansion yields the lowest quasienergy $E^* = gQ(\mathcal{X}_{min}, 0) + \frac{g}{2}\lambda\omega^*$ in the semiclassical limit as

$$E^* = -\frac{g}{4\lambda}\left(\frac{f}{g} + \frac{1}{2}\right)^2 + \frac{g}{2}\lambda\sqrt{\frac{2f}{g + 2f}}, \quad (4)$$

with the effective mass m^* being related to the effective frequency as $\omega^* = \sqrt{1/m^*} = \sqrt{2f/(g + 2f)}$. This result is correct up to $\mathcal{O}(\lambda^2)$ and is shown in Fig. 2c as orange dashed line. It almost coincides with the exact result, even for small photon numbers $N = 1$.

The groundstate $|\psi^*\rangle = R^{-1}D(\mathcal{X}_{min})S(r)|0\,g\rangle$ is obtained in terms of the Fock states in leading order in λ by applying to the vacuum $|0\,g\rangle$: i) the squeezing operator $S(r) = \exp\left[r(a^2 - a^{\dagger 2})/2\right]$ with squeeze factor $r = (\ln m^*)/4 = \ln[1 + g/(2f)]/4$, ii) the translation $D(\mathcal{X}_{\min}) = \exp[i\mathcal{P}\mathcal{X}_{\min}/\lambda]$ to the minimum, and iii) R^{-1} to switch back to the bare atom picture [15], i.e.,

$$|\psi^*\rangle \simeq \frac{e^{-|\alpha|^2(1-\nu/\mu)/2}}{\sqrt{\mu}}\left(|0\,g\rangle + \sum_{n=1}^{\infty}\frac{1}{\sqrt{2n!}}\left(\frac{\nu}{2\mu}\right)^{n/2}\right.$$
$$\left. \times H_n\left(\frac{\alpha}{\sqrt{2\nu\mu}}\right)\left(|n-1\,e\rangle - |n\,g\rangle\right)\right), \quad (5)$$

where $H_n(x)$ are the Hermite polynomials, $\nu = \sinh r$, $\mu = \cosh r$ and $\alpha = \mathcal{X}_{\min}e^r/\sqrt{2\lambda}$. Since $r > 0$, $D(\mathcal{X}_{min})S(r)|0\,g\rangle$ is an amplitude squeezed state.

With this at hand, we can readily compute expectation values in leading order, e.g., $A^* = |\langle\psi^*|a|\psi^*\rangle| = |\mathcal{X}_{\min}|/\sqrt{2\lambda} \simeq (f/g + 1/2)/2\lambda$, which is shown in Fig. 2, dashed orange line. Moreover, the mean photon number $\bar{n} = \langle\psi^*|n|\psi^*\rangle \simeq (f/g + 1/2)^2/4\lambda^2$ and variance $(\Delta n)^2 = \langle\psi^*|(n - \bar{n})^2|\psi^*\rangle \simeq e^{-2r}(f/g + 1/2)^2/4\lambda^2$. Hence, in the semiclassical limit $\lambda \to 0$, the 2-photon correlation function $g^{(2)}(0) \equiv 1 + ((\Delta n)^2 - \bar{n})/(\bar{n}^2) < 1$, implying that $|\psi^*\rangle$ has sub-Poissonian statistics and shows photon antibunching. When $\Delta n \gg 1$, the overlap of the Fock states and $|\psi^*\rangle$ changes slowly for varying n. Hence, one can replace $|n-1\,e\rangle$ by $|n\,e\rangle$ in Eq. (5) and, for $\lambda \to 0$, implying $\Delta n \gg 1$, obtain $|\psi^*\rangle \simeq (|e\rangle - |g\rangle)/\sqrt{2} \otimes D(\mathcal{X}_{min})S(r)|0\rangle$.

Next, we consider the dissipative semiclassical dynamics. As will be shown below, a separation of time scales exists which defines a fast intrawell and a slow interwell relaxation. Deep in the semiclassical limit, the quasienergy states, localized close to the minimum of one well, can be obtained as $|\psi_n^*\rangle = R^{-1}b^{\dagger n}R|\psi^*\rangle/\sqrt{n!}$ with $b = \mu a + \nu a^\dagger - \alpha$. In this limit, dissipative transitions occur only between nearest neighbors, with the rates

$\mathcal{L}_{n-1,n} = \gamma n \cosh^2 r$, $\mathcal{L}_{n,n-1} = \gamma n \sinh^2 r$. Here, the detailed balance condition is fullfilled. When the system is initially in a state with a large photon number, it has a large probability to fall in the basin of attraction of the quasipotential minimum (intrawell relaxation). When also $\gamma \ll g\lambda\omega^*$, detailed balance determines an effective Boltzmann distribution $P_n^* = P^* e^{-n\beta_{\mathrm{eff}}}$, with effective inverse temperature $\beta_{\mathrm{eff}} = 2\ln\coth r$. We emphasize that this link between the effective temperature and squeezing can be generalized to any driven quantum system with a smooth quasienergy surface and coupled linearly to a bath (e.g., the Duffing oscillator [10, 11, 12, 13] or the parametrically driven oscillator [9]). It can be easily generalized to finite temperatures $T > 0$ as well. It turns out that the zero temperature limit applies when $\sinh^2 r$ is much larger than the bosonic occupation number $\bar{n}(\omega_{\mathrm{ex}}/T)$ of the bath at ω_{ex}. In the opposite limit, $\beta_{\mathrm{eff}} = \omega_{\mathrm{ex}}/T$. Since we include here only photon leaking, i.e., $\omega_{\mathrm{ex}} \gg T$, the effective temperature is still small.

On the large time scale, the system decays to the 0-photon state with a rate k_- (interwell relaxation). From there, it can return to the basin of attraction of the minimum by a driving induced transition with a rate k_+. The stationary population of the intrawell states (oscillating out of phase) and the $0-$photon state (in phase) are determined by the ratio k_-/k_+. Away from resonance, photon leaking favors the $0-$photon state and $k_- \gg k_+$. Approaching a resonance, k_+ can increase up to Ω_N/π and can become comparable to k_-. Then, the response is qualitatively modified, as shown above. Here, the resonant-antiresonant transition is governed by the ratio k_-/Ω_N.

In the semiclassical regime, the smallest finite eigenvalue Γ of the Lindblad master equation consists of the sum of k_+ and k_- and is shown in Fig. 3b. The peaks are due to resonant tunneling from the 0- to N-photon state, whereas off resonance, $\Gamma \approx k_-$. There are three mechanisms of decay from the metastable well: (i) The system can decay directly to the 0-photon state with the rate shown in Fig. 3b, dashed-dotted orange line. (ii) The system can climb up the quasienergy well by quantum activation [8]. Both associated rates are expected to decrease exponentially, following $\propto e^{-c_i/\delta\omega^2}$, with some constants c_i (the prefactor varies smoothly with $\delta\omega$), which defines the separation of time scales. (iii) For very small detuning, the escape occurs via bath-induced spin-flips. In fact, this mechanism is suppressed only as a power-law $\Gamma \propto \delta\omega^2$. To separate (ii) from (iii), we show Γ without the bath-induced spin flips in Fig. 3b (dashed red line), illustrating that spin flips are dominant when the separation of time scales is well defined. Since only a few states close to the bottom are populated, our solution is stable against a small dephasing of the oscillator [9] or an intrinsic spin relaxation that violates detailed balance. The induced spin-flip rate would be small and remain finite for $\lambda \to 0$, imposing an upper limit to the lifetime of $|\psi^*\rangle$. We note that the real parts of the two eigenvalues corresponding to the dissipative and decoherence transition of $|\phi_{1+}\rangle \to |\phi_0\rangle$ are not included. They are approximately given by $\gamma/2$ and $\gamma/4$.

Our analysis can be easily extended to any driven nonlinear oscillator coupled bilinearly to a thermal bath. For example, the quantum Duffing oscillator is characterized by two classical stable solutions. For weak driving, the small-oscillation solution can be identified with the $0-$photon state. Since it is favored by photon leaking, it has a low effective temperature and can be regarded stable in absence of tunneling. However, the stable solution is associated to a relative quasienergy maximum, in contrast to static bistable potentials. At resonance, the solution becomes metastable, leading to a competition between tunneling out of the small oscillation state and the diffusion along the quasienergy surface [10, 12, 13].

In conclusion, inspired by recent experiments, we have explained the nonlinear response of the driven dissipative Jaynes-Cummings model. We have predicted the existence of a metastable squeezed state in the semiclassical limit and drawn a link between effective local temperature and the squeezing parameter. We have analyzed the escape mechanisms from the metastable states and found resonant dynamical tunneling. Our analysis reveals generic features on the dissipative dynamics of nonlinear driven quantum systems.

[1] E.T. Jaynes and F.W. Cummings, Proc. IEEE **51**, 89 (1963)
[2] J. Larson, Phys. Scr. **76**, 146 (2007).
[3] A. Wallraff *et al.*, Nature **431**, 162 (2004).
[4] I. Chiorescu *et al.*, Nature **431**, 159 (2004).
[5] N. Hatakenaka and S. Kurihara, Phys. Rev. A **54**, 1729 (1996).
[6] M. Winger *et al.*, Phys. Rev. Lett. **101**, 226808 (2008).
[7] L.S. Bishop *et al.*, Nature Phys. **5**, 105 (2009).
[8] M.I. Dykman and V.N. Smelyanskii, Sov. Phys. JETP **67**, 1769 (1989).
[9] M. Marthaler and M.I. Dykman, Phys. Rev. A **73**, 042108 (2006).
[10] V. Peano and M. Thorwart, Phys. Rev. B **70**, 235401 (2004).
[11] M.I. Dykman and M.V. Fistul, Phys. Rev. B **71**, 140508(R) (2005).
[12] V. Peano and M. Thorwart, Chem. Phys. **322**, 135 (2006).
[13] V. Peano and M. Thorwart, New J. Phys. **8**, 21 (2006).
[14] Y.T. Chough, H. Nha, and K. An, J. Phys. Soc. Jpn. **69**, 4060 (2000).

[15] H. P. Yuen, Phys. Rev. A **13**, 2226 (1976).